# *The Effective Static Stability Experienced by Eddies in a Moist Atmosphere*



**Citation:** O'Gorman, Paul A. "The Effective Static Stability Experienced by Eddies in a Moist Atmosphere." Journal of the Atmospheric Sciences 68.1 (2011) : 75-90. ©2011 American Meteorological Society

**As Published:** http://dx.doi.org/10.1175/2010jas3537.1

**Publisher:** American Meteorological society

**Persistent URL:** http://hdl.handle.net/1721.1/65826

**Version:** Final published version: final published article, as it appeared in a journal, conference proceedings, or other formally published context

# The Effective Static Stability Experienced by Eddies in a Moist Atmosphere

PAUL A. O'GORMAN

*Massachusetts Institute of Technology, Cambridge, Massachusetts*

(Manuscript received 26 April 2010, in final form 28 June 2010)

ABSTRACT

Water vapor directly affects the dynamics of atmospheric eddy circulations through the release of latent heat. But it is difficult to include latent heat release in dynamical theories because of the associated nonlinearity (precipitation generally occurs where there is upward motion). A new effective static stability is derived that fundamentally captures the effect of latent heat release on moist eddy circulations. It differs from the usual dry static stability by an additive term that depends on temperature and a parameter measuring the up–down asymmetry of vertical velocity statistics. Latent heat release reduces the effective static stability experienced by eddies but cannot reduce it to zero so long as there are nonprecipitating regions of the eddies. Evaluation based on reanalysis data indicates that the effective static stability in the lower troposphere ranges from ~80% of the dry static stability at high latitudes to ~25% in the tropics.

The effective static stability provides a solution to the longstanding problem of how to adapt dry dynamical theories to the moist circulations in the atmosphere. Its utility for climate change problems is illustrated based on simulations with an idealized general circulation model. It is shown to help account for changes in the thermal stratification of the extratropical troposphere, the extent of the Hadley cells, the intensity of extratropical transient eddies, and the extratropical eddy length.

## 1. Introduction

Much of our understanding of the general circulation of the atmosphere is based on dry dynamical theories that do not take account of the effect of latent heat release on circulations. While the importance of latent heat release has long been recognized in the case of tropical circulations, it is clear that latent heating must also strongly affect eddies in the subtropics and midlatitudes (Emanuel et al. 1987; Reed et al. 1988; Gutowski et al. 1992; Chang et al. 2002; Lapeyre and Held 2004). The need for an understanding of circulation changes associated with global warming makes a proper accounting of latent heat release more pressing, since the amount of water vapor in the atmosphere increases strongly with warming; zonal-mean column water vapor increases at a rate of 6% $K^{-1}$ to 12% $K^{-1}$ depending on latitude (O'Gorman and Muller 2010). The implied increases in latent heating are a potential driver of many of the expected changes in the dynamics of the atmosphere under global warming (Schneider et al. 2010).

There are many examples of dry dynamical theories that would be useful if applicable to the moist circulations of the atmosphere. These include the theory for the edge of the Hadley cell based on the supercriticality to baroclinic instability (Held 2000; Korty and Schneider 2008), the scaling of the extratropical eddy length with the Rossby deformation radius (e.g., Schneider and Walker 2006), and the use of growth rates of dry baroclinic instability to account for the position of extratropical storm tracks (Hall et al. 1994; Yin 2005). Dry theories are sometimes found to be adequate when applied to moist atmospheres (e.g., the use of dry mean available potential energy to explain changes in the intensity of extratropical eddies under climate change; O'Gorman and Schneider 2008a), whereas in other cases dry theories are found to perform poorly when applied to moist atmospheres (e.g., when applied to the extratropical thermal stratification; Thuburn and Craig 1997; Frierson 2008; Schneider and O'Gorman 2008). Even when dry theories are apparently successful in a moist atmosphere, it remains unclear why latent heating does not play a role, and this reduces our confidence in the resulting predictions.

It is difficult to include latent heat release in large-scale dynamical theories because condensation and precipitation are associated with saturated ascent but not

*Corresponding author address:* Paul A. O'Gorman, 77 Massachusetts Ave., Massachusetts Institute of Technology, Cambridge, MA 02139.
E-mail: pog@mit.edu

DOI: 10.1175/2010JAS3537.1

descent, so that the latent heating is a strongly nonlinear function of the dynamical fields. Latent heating introduces a Heaviside function into the dynamical equations, and while changing to a moist entropy thermodynamic variable (such as equivalent potential temperature) removes this nonlinearity from the thermodynamic equation, it remains in the equations governing water substance and precipitation. Only in the dry limit or in the limit in which it is "always raining" is this additional nonlinearity truly unimportant.

It is attractive to try to account for latent heat release by modifying the static stability, since the vertical velocity is both associated with latent heat release and multiplies the dry static stability in the thermodynamic equation (Kiladis et al. 2009). Bjerknes (1938) showed that the relevant static stability for moist convection is larger than a parcel argument would suggest if both the updraft and the subsiding environment are taken into account. In the case of tropical dynamics, effective static stabilities that account for latent heating have been introduced in terms of a precipitation efficiency (Yano and Emanuel 1991) or a gross moist stability based on a moist static energy budget (Neelin et al. 1987; Neelin and Held 1987). But the resulting dynamical theories for wave or eddy circulations are based on perturbations to an always-convecting atmosphere and so will not be generally applicable.

Lapeyre and Held (2004) assumed a form for an effective static stability based on an area-weighted average of dry and moist static stabilities and found that it helped explain the behavior of moist baroclinic eddies in a two-layer quasigeostrophic model. They also found that latent heating reduces the effective static stability, consistent with the need to reduce the mean static stability in order for dry simulations of midlatitude storm tracks to match observations (Chang 2006). The effective static stability of Lapeyre and Held (2004) seems promising in that it does not require an always-convecting atmosphere, but it is strongly tied to the moist two-layer quasigeostrophic model, and its physical basis is somewhat unclear because it was not derived from the underlying equations. The nonlinear association of precipitation with ascent must be addressed if such an effective static stability is to be derived from the moist dynamical equations.

Here, we derive a new effective static stability that takes account of the leading-order effects of latent heat release on eddy circulations and that does not neglect the association of precipitation with ascent (sections 2 and 3). The effective static stability is "effective" in the sense that it simultaneously takes account of the latent heating in regions of ascent and the dry static stability in regions of descent. It converts the moist primitive equations governing eddy dynamics to an equivalent set of dry primitive equations with a modified mean static stability term in the thermodynamic equation. We evaluate the effective static stability in the present climate using the National Centers for Environmental Prediction (NCEP)–Department of Energy (DOE) Reanalysis 2 dataset (NCEP-2; Kanamitsu et al. 2002) and discuss the extent to which latent heating reduces the effective static stability at different latitudes (section 4). Using a set of simulations with an idealized general circulation model (GCM) (section 5), we demonstrate that eddies governed by the dry primitive equations with the effective static stability have similar statistics to eddies in a full simulation with a hydrological cycle (section 6). We then go on to use the effective static stability to modify several dry analytical theories for different aspects of the general circulation and use the modified theories to account for changes in the general circulation in simulations with the idealized GCM over a wide range of climates (section 7). Our conclusions review the implications for the general circulation and include a brief discussion of the possible relevance to tropical wave dynamics (section 8).

## 2. Derivation of the effective static stability

We use the thermodynamics of saturated ascent to write an expression for the latent heating in terms of the vertical pressure velocity $\omega$ and the temperature. For an air parcel undergoing saturated ascent (e.g., pseudoadiabatic ascent) and conserving its saturated equivalent potential temperature $\theta^*$, the Lagrangian rate of change of dry potential temperature $\theta$ can be expressed as

$$\frac{D\theta}{Dt} = \omega \left.\frac{\partial \theta}{\partial p}\right|_{\theta^*} + \frac{D\theta^*}{Dt} \left.\frac{\partial \theta}{\partial \theta^*}\right|_{p} = \omega \left.\frac{\partial \theta}{\partial p}\right|_{\theta^*}, \qquad (1)$$

where we have used $\theta = \theta(p, \theta^*)$ and $D\theta^*/Dt = 0$. The expression for the latent heating rate on the far right-hand side of Eq. (1) has been used to successfully diagnose the dynamic and thermodynamic contributions to precipitation extremes in climate model simulations (O'Gorman and Schneider 2009a,b). We will assume that it continues to hold approximately even when other diabatic terms are present in the thermodynamic equation. We further make the simplifying approximation that condensation and latent heating occur if and only if the vertical velocity is upward ($\omega$ is negative). This will only be a good approximation to the extent that the distance to saturation (cf. O'Gorman and Schneider 2006) or before the onset of convection is small compared with the eddy length.

The terms in the Eulerian thermodynamic equation involving the vertical pressure velocity can then be written as[1]

[1] Partial derivatives are taken at fixed time and horizontal coordinates (e.g., $\partial\theta/\partial p$) unless otherwise noted (e.g., $\partial\theta/\partial p|_{\theta^*}$).

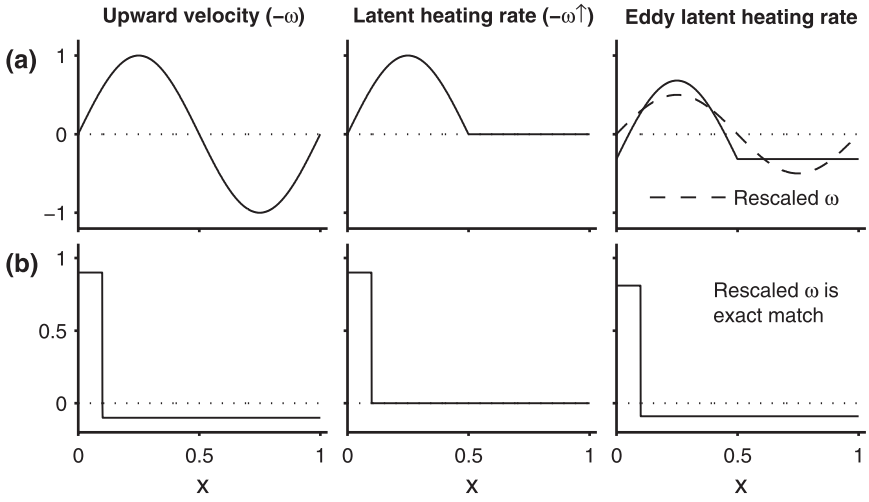


FIG. 1. Idealized vertical velocity profiles illustrating the derivation of the effective static stability. The profiles are plotted vs a spatial variable $x$ representative of longitude. Profiles are (a) sinusoidal and (b) constant in the ascent and descent regions with ascent over 10% of the domain. The profiles are chosen to have zero mean for simplicity. (left) The upward velocity $-\omega$. (middle) The truncated upward velocity $-\omega^{\uparrow}$, which is proportional to the latent heating rate. (right) The eddy truncated upward velocity $-\omega^{\uparrow\prime}$ (solid) and the approximation given by expression (4) (dashed). The rescaling coefficient $\lambda$ is 0.5 for (a) and 0.9 for (b). The normalized squared error given by Eq. (6) is $e^2 = 0.16$ for (a) and zero for (b).

$$\frac{\partial\theta}{\partial t} = -\omega\left[\frac{\partial\theta}{\partial p} - H(-\omega)\frac{\partial\theta}{\partial p}\bigg|_{\theta*}\right] + \cdots, \tag{2}$$

an expression that now holds for both ascent and descent, and where $H(\cdot)$ is the Heaviside function. The horizontal-advective and radiative terms in Eq. (2) are not written explicitly but have not been neglected. We are interested in the eddy dynamics, and so we need to write an equation for the evolution of the eddy potential temperature $\theta'$, with eddies defined relative to a zonal mean $\overline{\theta}$. Defining the truncated upward velocity as $\omega^{\uparrow} = H(-\omega)\omega$ and neglecting eddy variations in the pressure derivatives of potential temperature, we find

$$\frac{\partial\theta'}{\partial t} = -\omega'\frac{\partial\overline{\theta}}{\partial p} + \omega^{\uparrow\prime}\overline{\frac{\partial\theta}{\partial p}\bigg|_{\theta*}} + \cdots, \tag{3}$$

where the second term on the right-hand side is the eddy latent heating rate. The appendix discusses the accuracy of the approximations made so far in the representation of the latent heating term.

The central approximation of the derivation is to relate the eddy latent heating rate (or more precisely $\omega^{\uparrow\prime}$) to the eddy vertical velocity as follows:

$$\omega^{\uparrow\prime} = \lambda\omega' + \epsilon, \tag{4}$$

where $\epsilon$ is a residual, and a least squares estimate for the rescaling coefficient $\lambda$ is given by

$$\lambda = \frac{\overline{\omega'\omega^{\uparrow\prime}}}{\overline{\omega'^2}}, \tag{5}$$

with normalized squared error

$$e^2 = \frac{\overline{\epsilon^2}}{\overline{\omega^{\uparrow\prime 2}}}. \tag{6}$$

The essential insight motivating this approximation is that while the vertical velocity field cannot be rescaled to match the latent heating rate without leading to regions with large negative heating rates, the eddy latent heating rate does project strongly onto the eddy vertical velocity. Two simple examples of the approximation applied to idealized vertical velocity fields with zero mean are shown in Fig. 1. The first example (Fig. 1a) is a sine wave in which latent heating (proportional to $\omega^{\uparrow}$) occurs in half the domain, and the rescaled vertical velocity gives a relatively good match to the eddy latent heating rate. The second example (Fig. 1b) has a narrow updraft over 10% of the domain; the rescaled vertical velocity is an exact match for the eddy latent heating rate in this case. An observational example of the approximation is shown in Fig. 2 for a vertical velocity distribution at one time, latitude, and pressure level in the NCEP-2 reanalysis; its general accuracy is discussed in section 4. Note that the rescaling coefficient $\lambda$ is generally less than one because it takes account of the absence of latent heating in descent regions of the eddy.

The approximation of Eq. (3) governing the eddy potential temperature is then

$$\frac{\partial \theta'}{\partial t} = -\omega' \left( \frac{\partial \theta}{\partial p} \right)_{\text{eff}} + \cdots, \tag{7}$$

where the effective static stability is defined by

$$-\left( \frac{\partial \theta}{\partial p} \right)_{\text{eff}} = -\frac{\partial \theta}{\partial p} + \lambda \frac{\partial \theta}{\partial p}\bigg|_{\theta *}, \tag{8}$$

and we have dropped the zonal means for simplicity (whether the static stability or zonal mean of the static stability enters is immaterial at the level of the approximations made earlier). Equation (7) is the same as the dry thermodynamic equation, but with the static stability in the thermodynamic equation replaced by the effective static stability (8). The effective static stability may also be written in height rather than pressure coordinates if we assume changes in pressure and height are related hydrostatically, such that

$$\left( \frac{\partial \theta}{\partial z} \right)_{\text{eff}} = \frac{\partial \theta}{\partial z} - \lambda \frac{\partial \theta}{\partial z}\bigg|_{\theta *}, \tag{9}$$

where $\partial\theta/\partial z|_{\theta *} = -\rho g \partial\theta/\partial p|_{\theta *}$ and $\rho$ is density.

The effective static stability does not explicitly depend on mean humidity, and it cannot be derived by replacing the potential temperature with the equivalent potential temperature in the dynamical equations. Its utility beyond being a purely diagnostic quantity relies on the rescaling coefficient $\lambda$ being relatively constant, for example, with respect to latitude or under climate change, and the residuals in the approximation (4) being relatively small. This will turn out to be the case in the reanalysis data and model atmospheres considered in this study (see also the appendix).

## 3. Basic properties of the effective static stability

The effective static stability involves the dry static stability associated with a moist adiabatic stratification $\partial\theta/\partial z|_{\theta *}$. This thermodynamic function of temperature and pressure vanishes for sufficiently low temperatures, so that the effective static stability equals the dry static stability in the cold limit. In the limit of a moist adiabatic stratification, the effective static stability does not become zero but rather becomes a fraction $(1 - \lambda)$ of $\partial\theta/\partial z|_{\theta *}$. The effective static stability in the moist-adiabatic limit results from the nonzero dry static stability in descent regions of the eddies.

The mean vertical velocity influences the value of the rescaling coefficient $\lambda$. For a strongly upward mean vertical velocity, it is always precipitating and $\lambda = 1$. For a strongly downward mean vertical velocity, it is never precipitating and $\lambda = 0$. Asymmetries between ascent and descent also affect the value of $\lambda$. For zero-mean vertical velocity but nonzero skewness, we expect $0 \le \lambda \le 1$, with $\lambda > 0.5$ when there are stronger and narrower updrafts than downdrafts.

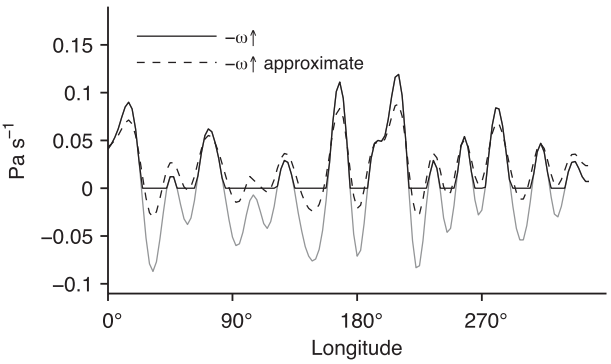


FIG. 2. Example from NCEP-2 reanalysis (60°S, 500 hPa, 1 Jan 1992) of the approximation (4) used in the derivation of the effective static stability: the instantaneous truncated upward velocity $-\omega^{\uparrow}$ (solid) and the approximation for $-\omega^{\uparrow}$ (dashed) that results from Eq. (4). The untruncated upward velocity $-\omega$ is shown in gray for reference. The value of $\lambda = 0.57$ is determined from the least squares estimate (5), with normalized squared error $\epsilon^2 = 0.18$. Full rather than eddy fields are shown for clarity.

The effective static stability (9) can be rewritten as a weighted average of a dry static stability $\partial\theta/\partial z$ and a moist static stability $\partial\theta^*/\partial z$ as

$$\left( \frac{\partial \theta}{\partial z} \right)_{\text{eff}} = (1 - \lambda) \frac{\partial \theta}{\partial z} + \lambda \frac{\partial \theta}{\partial \theta^*}\bigg|_{p} \frac{\partial \theta^*}{\partial z}, \tag{10}$$

where we have used

$$\frac{\partial \theta}{\partial p} = \frac{\partial \theta}{\partial p}\bigg|_{\theta *} + \frac{\partial \theta}{\partial \theta^*}\bigg|_{p} \frac{\partial \theta^*}{\partial p} \tag{11}$$

and the hydrostatic approximation. Remarkably, this resembles the effective static stability that was intuited by Lapeyre and Held (2004) in a two-layer quasigeostrophic model, except that we have an entirely different definition for the weighting $\lambda$. Lapeyre and Held (2004) interpreted $\lambda$ as an area fraction of precipitation and quantified it using an expression that involved the meridional moisture flux and the diffusivity of a moist potential vorticity. Our $\lambda$ is defined in terms of statistics of the vertical velocity, and it does not generally behave like the area fraction of precipitation (or ascent).

For example, in the case of zero-mean vertical velocity and constant vertical velocities in the ascent and descent regions of the eddies (cf. Fig. 1b), $\lambda$ is related to the updraft area fraction $a_u$ by $\lambda = 1 - a_u$, exactly opposite to the

interpretation of Lapeyre and Held (2004). Narrow intense updrafts $a_u \to 0$ correspond to $\lambda \to 1$ and relatively small effective static stabilities. This may seem surprising, since the dry static stability is then weighted by the updraft area fraction and the moist static stability is weighted by the downdraft area fraction. But it can be intuitively understood by realizing that small updraft areas correspond to intense updrafts that are largely unchanged by subtracting the mean of the truncated upward velocity, leading to a rescaling coefficient $\lambda \simeq 1$ (cf. Fig. 1b). Generalizing the piecewise constant vertical velocity distribution to have a mean vertical velocity $\overline{\omega}$, we find that

$$\lambda = \frac{1 - a_u}{1 - \overline{\omega}/\omega_u}, \tag{12}$$

where $\omega_u$ is the updraft velocity, and we have assumed that the mean vertical velocity is not strong enough to lead to only ascent or descent over the entire domain. Again we find that decreasing updraft area $a_u$ implies increasing $\lambda$.

The rescaling coefficient $\lambda$ does behave like the updraft area fraction in the case of a normally distributed vertical velocity, for which the skewness is fixed at zero, and $\lambda = a_u$ consistent with Lapeyre and Held (2004). But the skewness of vertical velocities in the atmosphere varies and is not generally zero (eddy vertical velocities are not symmetric between up and down). In fact, the effective static stability derived here may more closely resemble the effective static stability implied by the Bjerknes "slice method" for moist convection, in which the updraft area fraction also multiplies the dry static stability (Bjerknes 1938; Emanuel 1994).

## 4. Evaluation based on reanalysis data

We evaluate the effective static stability in the present climate using NCEP-2 reanalysis data from 1992–2001 (Kanamitsu et al. 2002). The spatial resolution is 2.5° and 4-times-daily data are used. Our results are based on a zonal and time mean, but the effective stability could in principle be generalized so that it also varies in longitude (e.g., by using a time mean).

The effective static stability explicitly depends on vertical velocity statistics through the rescaling coefficient $\lambda$. As calculated from the reanalysis data, this is relatively homogeneous throughout the extratropical troposphere, with values $\lambda \simeq 0.55$ (Fig. 3a). Given the small mean vertical velocities in the extratropics, $\lambda$ values somewhat greater than 0.5 imply that the eddy vertical velocity distribution is slightly skewed toward stronger and narrower updrafts than downdrafts. Indeed, the area fraction of updrafts is generally less than 0.5, with typical values of

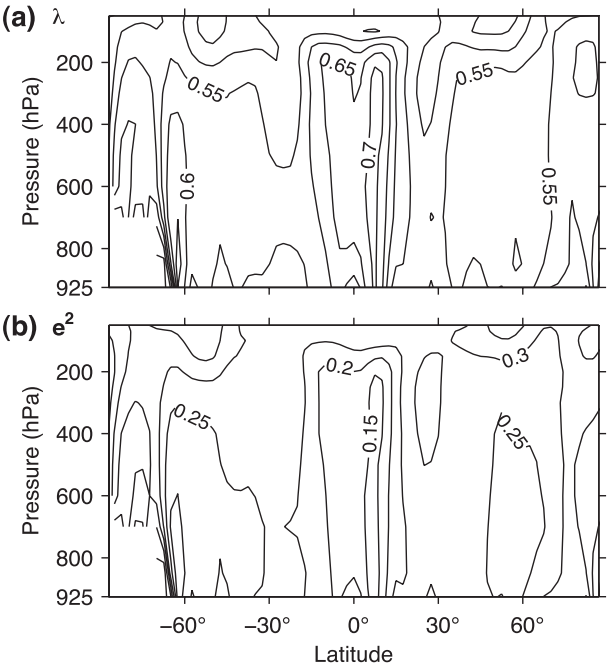


FIG. 3. (a) The rescaling coefficient $\lambda$ in approximation (4) based on NCEP-2 reanalysis (1992–2001); (b) the normalized squared error $e^2$. The eddy vertical velocity and the averages denoted by an overbar in Eq. (4) are calculated based on a zonal and time average. Values at the 1000-hPa level are not shown to avoid difficulties with subsurface values.

$\sim$0.45, roughly consistent with Eq. (12). Values of $\lambda$ in the deep tropics are larger ($\lambda \simeq 0.7$) in part because of the strong mean ascent, whereas there is a slight local minimum in $\lambda$ in the region of mean descent in the subtropics. The normalized squared error associated with the approximation (4) ranges from $e^2 \simeq 0.15$ to 0.3, with generally larger values at higher latitudes (Fig. 3b). In the extratropics, the normalized squared error $e^2$ is close to the value of 0.27 that would be obtained from a normally distributed vertical velocity with zero mean (a completely inaccurate approximation corresponds to $e^2 = 1$). These relatively small residuals imply that the central approximation used in deriving the effective static stability is sufficiently accurate to capture the primary effects of latent heat release on the eddy dynamics.

We next consider the distribution of the effective static stability and how much it is reduced compared with the dry static stability. The effective static stability (9) is evaluated based on the zonal and time mean temperatures and the rescaling coefficient $\lambda$ calculated as above. We present our results in terms of the square of the buoyancy frequency, calculated in the case of the effective static stability as $N^2_{\text{eff}} = (g/\theta)(\partial\theta/\partial z)_{\text{eff}}$, with the corresponding expression for the dry buoyancy frequency squared $N^2$ obtained by replacing the effective static stability with the

dry static stability. While $N^2$ does not vary strongly with latitude in the midtroposphere (Fig. 4a), $N^2_{\text{eff}}$ has a considerably smaller value in the tropics than at high latitudes (Fig. 4b). The ratio of the effective to the dry buoyancy frequency squared ($N^2_{\text{eff}}/N^2$) makes clear that the fractional reduction in static stability is largest at lower levels and lower latitudes (Fig. 4c); this reflects the distribution of water vapor in the atmosphere and the relatively constant values of the rescaling coefficient $\lambda$. Interestingly, the reduction in buoyancy frequency squared in the deep tropics (by a factor of 3–5 in the middle and lower troposphere) is close to being consistent with the observed reduction in equivalent depth of convectively coupled versus dry equatorial waves (Wheeler and Kiladis 1999; Kiladis et al. 2009), and the relevance to tropical waves is discussed further in the conclusions. Note also in this context that the effective static stability may be somewhat too large in the tropics because of the possible underestimation of latent heating rates discussed in the appendix.

The reduction in static stability is still considerable at midlatitudes (~40% in the lower troposphere at 50° latitude in both hemispheres). An important implication is that in addition to enabling a substantial amount of the extratropical poleward energy transport (Trenberth and Stepaniak 2003), latent heat release also strongly influences eddy dynamics in the extratropics of the current climate.

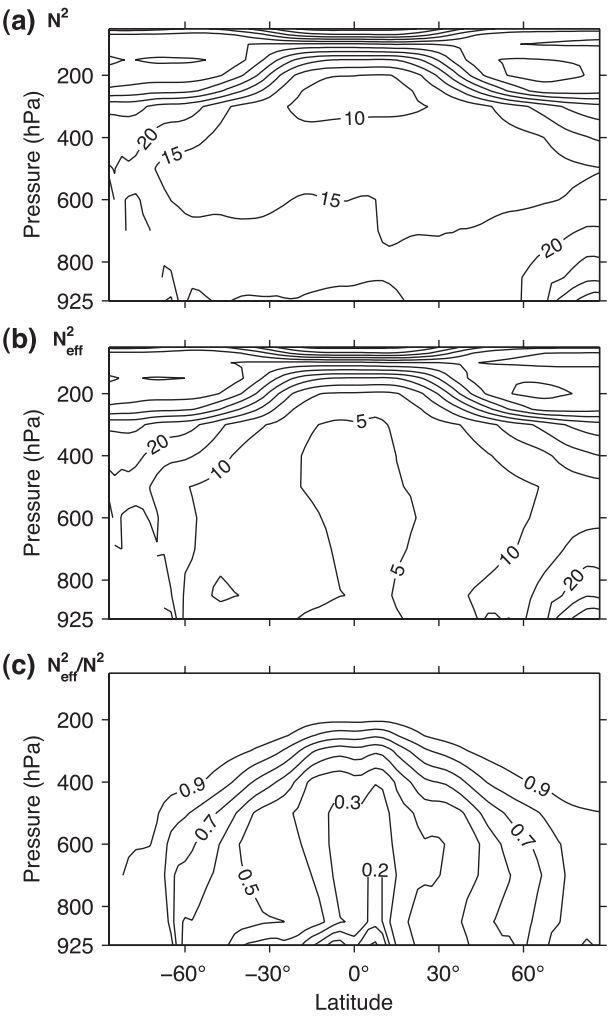


FIG. 4. (a) The dry buoyancy frequency squared, $N^2$ ($10^{-5}$ s$^{-2}$). (b) The effective buoyancy frequency squared, $N^2_{\text{eff}}$($10^{-5}$ s$^{-2}$). (c) The ratio of the effective to the dry buoyancy frequency squared, $N^2_{\text{eff}}/N^2$. Values are based on zonal and time mean temperatures in the NCEP-2 reanalysis (1992–2001).

## 5. Idealized GCM simulations

Simulations with an idealized GCM will be used in section 6 to directly test the effective static stability and in section 7 to show how the effective static stability can be used to account for the effect of climate change on the general circulation. The idealized GCM is based on the atmospheric dynamical core of the Geophysical Fluid Dynamics Laboratory (GFDL) climate model, but with simplified parameterizations of radiation and moist processes (Frierson 2007; O'Gorman and Schneider 2008b). The lower boundary is a mixed layer ocean with no horizontal energy transports or sea ice, and the statistics of the resulting simulations are zonally symmetric. The mixed layer is shallow (0.5 m in depth) in order to speed convergence. A semigray radiation scheme is used for longwave radiation, and fixed shortwave fluxes are imposed with no seasonal or diurnal cycle. A relatively simple parameterization is used for moist convection (Frierson 2007), and there is no ice or clouds. All simulations are run to statistical equilibrium and time averages are taken over a subsequent 300-day period.

A wide range of climates is generated by multiplying a reference longwave optical depth distribution by a constant $\alpha$ that varies from 0.4 to 6.0 in a range of different simulations. These simulations have been discussed in detail in O'Gorman and Schneider (2008a,b), Schneider and O'Gorman (2008), and Schneider et al. (2010). The $\alpha = 0.2$ simulation discussed in some previous papers is omitted here because the ambiguous nature of the extratropical tropopause in this simulation (cf. Fig. 1 of O'Gorman and Schneider 2008a) makes some of the results of section 7 sensitive to the definition of the tropopause. The reference simulation with $\alpha = 1$ has the climate that is most similar to present-day earth, and this is the parameter choice for the test of the effective static stability in section 6. The idealized GCM uses a $\sigma$ coordinate in the vertical, and so the effective static stability is calculated using a surface pressure weighting when calculating averages.

The tropopause height increases as the climate warms in the idealized GCM. But averaged over the depth of the

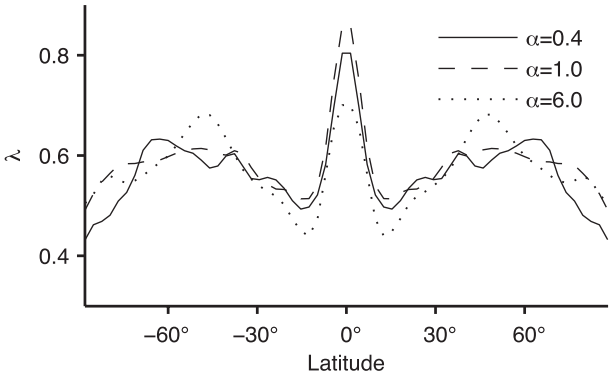


FIG. 5. The rescaling coefficient $\lambda$ in three simulations with the idealized GCM: the coldest simulation $\alpha = 0.4$ (solid), the reference simulation $\alpha = 1.0$ (dashed), and the warmest simulation $\alpha = 6.0$ (dotted). The eddy vertical velocity and the averages denoted by an overbar in Eq. (5) were calculated based on a zonal and time average. Averages were then taken from the surface to the tropopause at each latitude (the level at which the zonal- and time-mean temperature lapse rate is 2 K km$^{-1}$). An interhemispheric average was also taken, and a 1–2–1 filter in latitude was applied to the results for clarity.

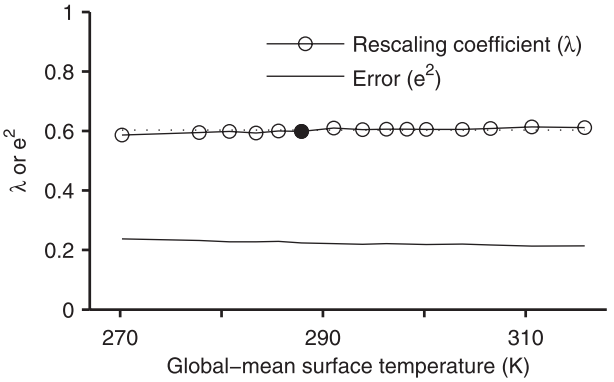


FIG. 6. The rescaling coefficient $\lambda$ (solid lines and circles) and normalized squared error $e^2$ (solid line) over a wide range of climates simulated with the idealized GCM. Extratropical (excluding latitudes equatorward of 30° in both hemispheres) and vertical–tropospheric averages are shown. The filled circle indicates the reference simulation, and the dotted line shows the mean value of $\lambda$ over all the simulations (0.60). The values of $\lambda$ in the coldest and warmest simulations are 0.59 and 0.61, respectively. The normalized squared error $e^2$ also varies little over the range of climates, with a mean of 0.22 and values in the coldest and warmest climates of 0.24 and 0.21, respectively.

troposphere, the rescaling coefficient $\lambda$ that appears in the definition of the effective static stability is found to be close to constant over a wide range of climates (global-mean surface air temperature ranging from 270 to 316 K), as shown in Figs. 5 and 6. The values of $\lambda$ and the normalized squared error $e^2$ are quite similar to those based on the NCEP-2 reanalysis (Fig. 3). The almost constant values of $\lambda$ as the climate changes make the effective static stability particularly useful for understanding changes in circulations under climate change.

## 6. Demonstration of validity

We now demonstrate that the effective static stability captures the primary effects of latent heat release on eddy statistics in the reference ($\alpha = 1$) simulation with the idealized GCM. Our method is to compare eddy statistics in the moist simulation and in corresponding dry simulations in which the static stability is replaced by the effective static stability.

Because the effective static stability only applies to the eddy dynamics, we use a special type of simulation in which the zonal-mean fields are held fixed. The zonal-mean fields are initialized from the 300-day time average of the corresponding fully dynamical simulation and held steady by zeroing the lowest zonal Fourier mode in the tendency terms. The zonal mean that is held fixed is therefore along $\sigma$ surfaces but without surface-pressure weighting. We do not hold the zonal-mean specific humidity fixed since this is not necessary to make a proper comparison.

We will refer to the simulation with time-varying zonal-mean fields and a hydrological cycle as the "full" simulation, the simulation with fixed zonal-mean fields and a hydrological cycle as the "fixed-moist" simulation, and the dry simulations with fixed zonal-mean fields and an effective static stability as the "fixed-effective" simulations. Atmospheric water vapor does not affect radiative fluxes in the idealized GCM, which facilitates the comparison between the fixed-moist and fixed-effective simulations.

Several modifications are needed to implement the fixed-effective simulation. First, the moist convection and large-scale condensation parameterizations are turned off. Second, the surface energy budget must be modified so that the results are not potentially distorted by large changes in the surface fluxes in the absence of a hydrological cycle. This is accomplished by maintaining a pseudoevaporation term in the surface energy budget used to evolve the mixed layer temperature forward in time. The pseudoevaporation term was calculated in the same way as in the full simulation using a bulk-aerodynamic formula, except that because there is no longer a lowest-level relative humidity available for the calculation, we instead use a fixed lowest-level relative humidity set equal to the time- and global-mean value in the full simulation (73%). Finally, the thermodynamic equation must be modified to account for the effective static stability following Eqs. (7) and (8). In practice, this involves adding an extra term $\omega\lambda(T/\theta)\partial\theta/\partial p|_\theta *$ to the temperature tendency. For simplicity, we evaluate the extra term in the thermodynamic equation using the local and instantaneous

temperature, and we use a globally constant value of $\lambda$ at all levels, latitudes, and longitudes. To test the validity of the expression (5) for $\lambda$, the fixed-effective simulations are performed for a range of $\lambda$ values from 0 to 1.

The eddies in the simulations with fixed zonal-mean fields equilibrate and reach amplitudes comparable to eddies in the full simulation. Eddies generally equilibrate through a combination of nonlinear eddy–eddy interactions, eddy–mean interactions, and dissipative processes. In the absence of eddy–mean interactions, it is still possible for eddies to equilibrate through the other two processes. The numerical stability of the simulations is, however, reduced by holding the zonal-mean fields fixed. Simulations with other values of the radiative parameters and fixed zonal-mean fields were found to eventually become numerically unstable. This instability seems to be related to stratospheric winds and could be delayed or suppressed by not holding fixed the zonal-mean fields in the stratosphere. The equilibration of the eddies with fixed zonal-mean fields provides an interesting counterpoint to a previous study in which mean fields were allowed to vary but eddy–eddy interactions were suppressed and the eddies were also found to equilibrate, albeit at higher amplitudes than in a fully dynamical simulation (O'Gorman and Schneider 2007).

We present our comparison of the different types of simulations in terms of the global-mean eddy kinetic energy (EKE), which is dominated by extratropical eddies. Eddies are defined relative to the zonal and time mean for the purposes of calculating the EKE. The global-mean EKE in the fixed-moist simulation is 0.63 MJ $m^{-2}$, which is very similar to its value of 0.60 MJ $m^{-2}$ in the full simulation. However, the global-mean EKE in the fixed zonal-mean simulation when the effective static stability is not used ($\lambda = 0$) is 0.07 MJ $m^{-2}$, a factor of 9 lower than in the fixed-moist simulation, consistent with the conclusions of Chang (2006). More generally, increasing $\lambda$ increases the EKE (Fig. 7), indicating that latent heat release strongly increases the amplitude of eddies for fixed mean fields. Interpolation of the results shown in Fig. 7 implies that the amplitude of the eddies would be the same in the fixed-moist and fixed-effective simulations for a value of $\lambda = 0.64$, which is close to the value of $\lambda \simeq 0.6$ given by expression (5) (cf. Fig. 5). The slightly higher value of $\lambda$ needed to give the correct eddy energies may be related to the possible underestimation of latent heating by the preliminary approximations in the derivation of the effective static stability (see the appendix). Eddy statistics as a function of latitude and pressure are also reproduced quite accurately in the fixed-effective simulations for $\lambda = 0.64$, with the greatest discrepancies at low latitudes, as demonstrated for the meridional wind variance in Fig. 8.

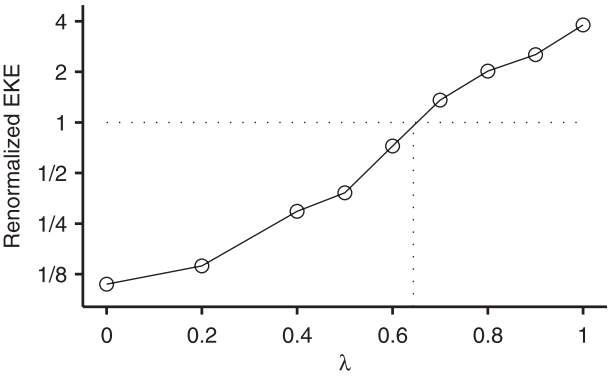


FIG. 7. Global EKE in simulations with fixed zonal-mean fields, no hydrological cycle, and the effective static stability (the fixed-effective simulations) for a range of values of the coefficient $\lambda$ in the definition of the effective static stability. The values are renormalized by the global EKE in the fixed-moist simulation (which does have a hydrological cycle). The fixed-effective simulation replicates the fixed-moist simulation's global EKE for a value of $\lambda \simeq 0.64$ (dotted lines). The dry simulation ($\lambda = 0$) has a global EKE that is 9 times too small. Note the log scale in the vertical axis.

These results make clear that latent heating strongly affects eddy equilibration for a given mean state (the EKE being almost an order of magnitude too small if latent heating is completely neglected). This does not mean that a similarly large difference in eddy energies between dry and moist simulations would result if the mean fields were allowed to equilibrate differently in each simulation. Rather, the important conclusions of this section are that replacement of the hydrological cycle by the effective static stability leads to the correct amplitude of equilibrated eddies for a given mean state, and that expression (5) gives roughly the correct value for $\lambda$.

## 7. Application to climate change problems

Several features of the general circulation of the atmosphere are expected to change in response to climate change. Here, we show that the effective static stability helps account for changes in four of these features, namely the extratropical thermal stratification, the extent of the Hadley cells, the intensity of extratropical transient eddies, and the extratropical eddy length. The successful application of the effective static stability in this wide range of problems illustrates its usefulness for understanding the moist general circulation and its response to climate change.

### *a. Thermal stratification of the extratropical troposphere*

The response of the extratropical thermal stratification to climate change is important for a number of reasons, including the radiative lapse-rate feedback. Several

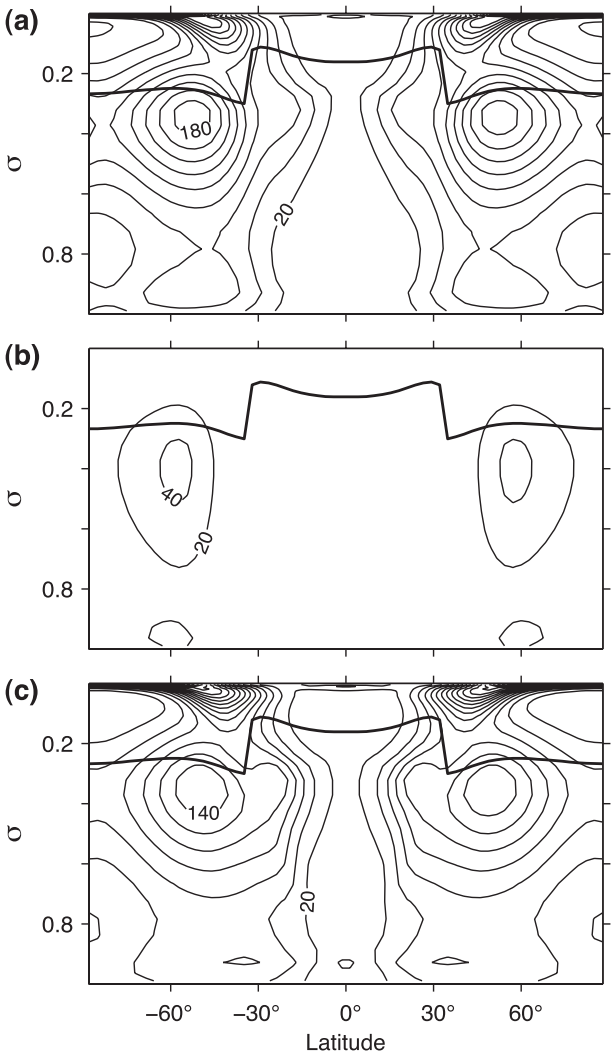


FIG. 8. Comparison of the variance of the meridional wind ($m^{-2}$ $s^{-2}$) in simulations with fixed zonal-mean fields and (a) a full hydrological cycle (the fixed-moist simulation), (b) no hydrological cycle, and (c) no hydrological cycle but with the effective static stability (the fixed-effective simulation). The effective static stability is evaluated using $\lambda = 0.64$ (cf. Fig. 7), which is close to the value of ~0.6 given by Eq. (5) in the extratropics. Zonal, time, and interhemispherically averaged fields are shown; the thick line is the tropopause. The radiative parameter is $\alpha = 1$ in all cases, corresponding to the reference simulation.

theories have been proposed to relate the thermal stratification to the meridional temperature gradient, including baroclinic adjustment theories (e.g., Stone 1978; Gutowski 1985; Zurita-Gotor and Lindzen 2007) and a theory based on diffusive fluxes of potential vorticity that results in a formally similar constraint on the stratification (Schneider and Walker 2006). These dry theories have been shown to be inadequate in moist atmospheres (Thuburn and Craig 1997; Schneider and O'Gorman 2008; Frierson 2008). An alternative theory that posits a central role for moist convection in maintaining a minimum static stability does take latent heating into account (Juckes 2000) and gives better results in moist atmospheres (Frierson 2008) but has been found to give poor results when tested in detail (Schneider and O'Gorman 2008). Nonetheless, the totality of these previous studies suggests that a dynamical constraint that relates the thermal stratification to the meridional temperature gradient may exist, but it must allow for the effects of latent heat release.

Here we show that a modified version of the supercriticality constraint of Schneider and Walker (2006) (in which the effective static stability replaces the dry static stability) accounts for the changes in the extratropical thermal stratification in the idealized GCM simulations. We also find good agreement when the supercriticality constraint is based on baroclinic adjustment theory in terms of the midtropospheric effective static stability and meridional temperature gradient [consistent with, say, the two-level model results of Zhou and Stone (1993)] (not shown). The justification for the use of the effective static stability in baroclinic adjustment theories is straightforward, since such theories are phrased in terms of a neutral state to growth of baroclinic eddies. A justification for modifying the theory of Schneider and Walker (2006) using the effective static stability might involve the introduction of a new potential temperature coordinate as the vertical integral of the effective static stability and subsequent verification of the validity of several approximations made in the original theory. We choose to present our results in terms of the supercriticality formulation of Schneider and Walker (2006) in part because it has been tested extensively in dry GCMs, but note that both classes of theory yield formally similar supercriticality constraints.

The dry static stability $-\overline{\partial\theta/\partial p}^{s}$ is evaluated near the surface following the conventions in Schneider and Walker (2006), and we take extratropical averages over the baroclinic zones in each hemisphere, defined as in O'Gorman and Schneider (2008a).[2] The precise averaging

[2] All quantities are calculated based on zonal, time, and interhemispherically averaged fields, denoted by $\overline{(\cdot)}$. The baroclinic zones are defined as the regions within 15° latitude of the extremum in the vertically integrated eddy potential temperature flux. The vertical integral of the eddy potential temperature flux is mass weighted and performed from the surface to the lowest level of the tropopause. The tropopause is defined as the level at which the zonal- and time-mean lapse rate is 2 K $km^{-1}$. Following Schneider and Walker (2006), the near-surface quantities are generally calculated above the boundary layer as the vertical average from $\sigma = 0.8$ to 0.7, and the pressure depth of the troposphere is calculated as the pressure difference from the tropopause to $\sigma = 0.75$. But the near-surface dry static stability used to define the supercriticality is evaluated as $\overline{\partial\theta/\partial z}^{\sigma}/(\overline{\rho}_s g)$, where $\overline{(\cdot)}^{\sigma}$ denotes a vertical average from $\sigma = 0.8$ to 0.7, and $\overline{\rho}_s$ is the mean density at the lowest model level. The near-surface moist adiabatic stability $-\overline{\partial\theta/\partial p|_{\theta^*}}^{s}$ is evaluated in a similar way for consistency.

conventions used are chosen for consistency with previous work. The extratropical dry static stability changes nonmonotonically as the climate warms, with a minimum close to the reference climate (which is closest to that of the present-day earth) and larger values in very cold or warm climates (Fig. 9).

The dry theory holds that a supercriticality $S$ defined in terms of the thermal structure of the atmosphere is a constant of order 1. The introduction of the effective static stability into the dry theory yields a modified expression for an effective supercriticality,

$$S_{\text{eff}} = f\frac{\overline{\partial\theta}^{s}}{\partial y}\left[2\beta\Delta_p\left(\frac{\overline{\partial\theta}^{s}}{\partial p}\right)_{\text{eff}}\right]^{-1}, \tag{13}$$

where $\Delta_p$ is the zonal- and time-mean pressure depth of the troposphere, $\partial\overline{\theta}^{s}/\partial y$ is the near-surface meridional temperature gradient, and the Coriolis parameter $f$ and its meridional gradient $\beta$ are evaluated at the center of the baroclinic zone. Substitution of the effective static stability (8) and rearrangement yields an expression for the dry static stability in a moist atmosphere:

$$-\frac{\overline{\partial\theta}^{s}}{\partial p} = -\lambda\frac{\overline{\partial\theta}^{s}}{\partial p}\bigg|_{\theta*} - \frac{f}{2\beta S_{\text{eff}}\Delta_p}\frac{\overline{\partial\theta}^{s}}{\partial y}. \tag{14}$$

In evaluating Eq. (14), we first take averages of the static stabilities, surface meridional temperature gradient, and pressure depth of the troposphere over the baroclinic zones.

The estimate of the dry static stability appropriate for dry atmospheres is recovered from Eq. (14) in the cold limit in which $\partial\theta/\partial p|_{\theta*}$ vanishes, or by setting $\lambda = 0$ at any temperature. This dry estimate (setting $\lambda = 0$) is plotted in Fig. 9, where we have chosen the value of the dry supercriticality $S = 0.9$ to give the best fit to the actual dry static stability in the simulations. In the colder climates, both the dry static stability and the dry estimate decrease as the climate warms. But in the warmer climates, the dry static stability increases with warming, whereas the dry estimate continues to decrease because of the increasing depth of the troposphere and decreasing near-surface meridional temperature gradients (cf. O'Gorman and Schneider 2008a).

The estimate using the effective static stability (14) is in much better agreement at all temperatures (Fig. 9), where we have again chosen the supercriticality constant to give the best fit ($S_{\text{eff}} = 1.4$). We have used a constant value of $\lambda = 0.6$ that is typical of the extratropics (Fig. 5); similar results are obtained if $\lambda$ is allowed to vary with latitude and pressure and between simulations. The

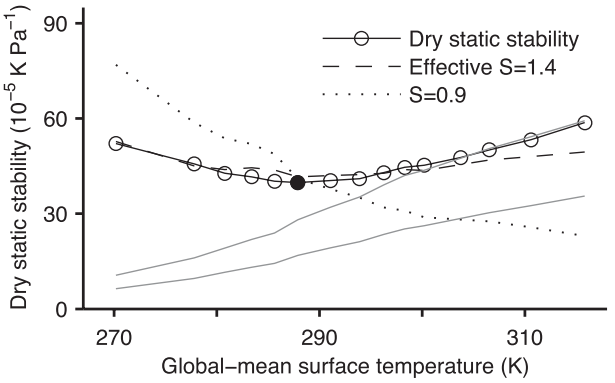


FIG. 9. Extratropical dry static stability over a wide range of climates in the idealized GCM (solid line and circles), and its predicted value from an effective supercriticality constraint $S_{\text{eff}} = 1.4$ (dashed), and from a dry supercriticality constraint $S = 0.9$ (dotted). The lower gray line shows the latent heating contribution to the effective supercriticality prediction [the first term on the right-hand side of Eq. (14)], and the upper gray line shows the dry static stability that would result from a moist adiabatic stratification. The constant supercriticality values are determined by a least squares fit of the resulting dry static stabilities. A constant value of $\lambda = 0.6$ is used in the effective supercriticality calculation. The reference simulation is shown with a filled circle in Figs. 9–12.

contribution of latent heat release [the first term on the right-hand side of Eq. (14)] is plotted as the lower gray line; it steadily increases with increasing temperature. The combination of the two terms on the right-hand side of Eq. (14) explains the U-shaped dependence of the dry static stability on global-mean surface temperature.

In the warmest climates (global-mean surface temperatures in excess of ~300 K), the dry static stability becomes equal to that given by a moist adiabat (upper gray line in Fig. 9), which is more stable than the prediction from the effective supercriticality (14). This corresponds to a transition from a combination of eddies and moist processes controlling the thermal stratification to moist convection alone controlling the thermal stratification.[3] The transition occurs at a higher global-mean surface temperature when the stratification in the midtroposphere is considered (not shown). A similar transition occurred in the dry simulations of Schneider and Walker (2006) in which the convection scheme relaxed temperatures to a subadiabatic lapse rate to mimic moist convection. But it could not occur in the theoretical framework of Juckes (2000) except in the trivial limits of no eddy activity or meridional entropy gradient. The

[3] The effective supercriticality decreases in the very warm climates in which moist convection controls the stratification; it decreases by a factor of 1.7 from the coldest to the warmest simulation, compared with a factor of 3.8 for the dry supercriticality.

exact temperature at which the transition occurs in the earth's atmosphere would likely vary seasonally and between hemispheres, and warrants further investigation.

### b. Extent of the Hadley cells

An expansion of the Hadley cells is found to occur in simulations of global warming scenarios (Lu et al. 2007) and is also found in observational trends in recent decades (Seidel et al. 2008). Held (2000) argued that the poleward edges of the Hadley cells correspond to the latitudes of onset of baroclinic instability, and that these latitudes are associated with a certain value of the supercriticality to baroclinic instability. Korty and Schneider (2008) made a somewhat different argument in terms of the vertical extent of eddy heat fluxes, but with a similar result that the supercriticality has a constant value of $S = 0.6$ at the poleward edges of the Hadley cells in dry atmospheres. If the dry arguments are applied without modification to a moist atmosphere, then it is unsurprising that the Hadley cells should expand with warming, since the dry static stability and tropopause height are expected to increase with warming. But the increase in dry static stability is often linked to the increase in dry static stability associated with a moist adiabat, and this is clearly unsatisfactory since the increasing latent heat release has been taken into account in the moist adiabat but not in the supercriticality constraint.

The Hadley cells expand with warming in the idealized simulations over most of the range of climates (Fig. 10). Following Korty and Schneider (2008) and applying a dry supercriticality constraint of $S = 0.6$ [calculated by using the dry static stability in expression (13)] yields latitudes for the poleward edges of the Hadley cell that are much too far poleward. But using a different dry supercriticality constant $S = 0.3$ gives reasonably good agreement, except in the very warmest climates (Fig. 10). Thus, the dry theory seems to be performing adequately if we are allowed to choose a different supercriticality constant in a moist atmosphere. Given the importance of latent heating in the subtropics, it is not clear why the dry theory seems to be adequate, but this mystery is resolved by the effective static stability.

The effective supercriticality constraint $S_{\text{eff}} = 0.6$ is found to also give reasonably good agreement for the poleward edges of the Hadley cells (Fig. 10). We have used $\lambda = 0.5$ based on its typical values at the poleward edge of the subtropics (cf. Fig. 5). The agreement with the supercriticality value of 0.6 found for dry atmospheres (Korty and Schneider 2008) is notable, and the effective supercriticality constraint for the poleward edges of the Hadley cells provides a more consistent theory than simply applying the dry theory in the hope that moisture does not matter.

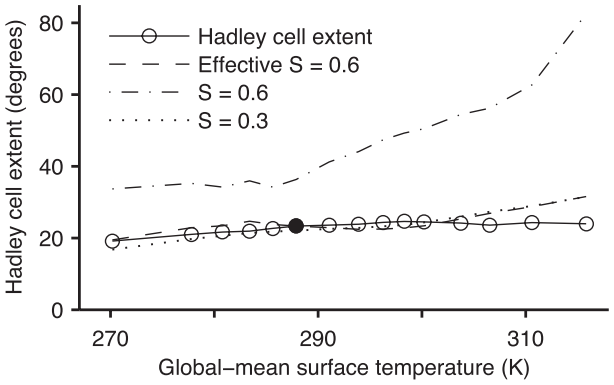


FIG. 10. The latitude of the poleward edge of the Hadley cell over a wide range of climates in the idealized GCM (solid line and circles), and its predicted value from an effective supercriticality constraint $S_{\text{eff}} = 0.6$ (dashed), and two dry supercriticality constraints $S = 0.6$ (dashed–dotted) and $S = 0.3$ (dotted). The edge of the Hadley cell is diagnosed following Korty and Schneider (2008) as the first latitude poleward of the maximum absolute value of the streamfunction above $\sigma = 0.7$ at which (at the $\sigma$ level of the maximum) its absolute value is 10% of the maximum value. A constant value of $\lambda = 0.5$ is used in the effective supercriticality calculation.

The effective static stability also explains why the dry theory seems to be adequate with a modified supercriticality constant of $S = 0.3$. Since the thermal stratification at the edge of the subtropics is generally close to (but not) moist adiabatic, the effective static stability (9) at the poleward Hadley cell edges is approximately

$$\left(\frac{\partial\theta}{\partial z}\right)_{\text{eff}} \simeq (1-\lambda)\left.\frac{\partial\theta}{\partial z}\right|_{\theta^*}, \tag{15}$$

so that the dry supercriticality is roughly half the effective supercriticality at the poleward edges of the Hadley cells.

The deviation of the Hadley cell extent from the effective supercriticality prediction in very warm climates (Fig. 10) is similar to the deviation of the dry static stability from its effective supercriticality estimate in very warm climates (Fig. 9). Both may relate to a transition in whether eddies play a role in setting the local static stability. In the case of the Hadley cell, the transition could alternatively relate to whether upper-tropospheric eddy momentum fluxes are dynamically important (see Fig. 6 of Schneider et al. 2010). We also find narrower than predicted Hadley cells in simulations with small meridional insolation gradients (not shown).

### c. Intensity of extratropical transient eddies

Studies of the effect of climate change on the extratropical storm tracks have come to mixed conclusions regarding changes in intensity. Some studies focused on cyclone statistics conclude that the overall frequency of

cyclones decreases in response to global warming but that the frequency of strong cyclones increases (e.g., Geng and Sugi 2003), while other studies conclude that there is little change in cyclone statistics (e.g., Bengtsson et al. 2009). A different approach based on the scaling of EKE with mean available potential energy (MAPE) has been used to relate changes in the intensity of extratropical transient eddies to changes in the mean temperature distribution. This energetic approach has been applied successfully to changes in the storm tracks in simulations with both dry and moist idealized GCMs (Schneider and Walker 2008; O'Gorman and Schneider 2008a). The extratropical EKE in the idealized GCM simulations is maximum in a climate close to the reference climate, with smaller values in very warm or cold climates (Fig. 11).[4] The changes in EKE are consistent with linear scaling with dry MAPE, and the reasons for the nonmonotonic changes in dry MAPE with warming are discussed in O'Gorman and Schneider (2008a).

Here, we introduce an effective MAPE that accounts for latent heat release by replacing the static stability with the effective static stability in Lorenz's quadratic approximation for the dry MAPE (Lorenz 1955). The effective MAPE per unit area is calculated as

$$\mathrm{MAPE}_{\mathrm{eff}} = \frac{c_p \kappa}{2g} \int_{0.9}^{\sigma_t} d\sigma \frac{\langle \overline{p} \rangle^{\kappa-1} (\langle \overline{\theta}^2 \rangle - \langle \overline{\theta} \rangle^2)}{p_0^{\kappa-1} \left\langle \left( \frac{\partial \overline{\theta}}{\partial p} \right)_{\mathrm{eff}} \right\rangle}, \quad (16)$$

where $\langle \cdot \rangle$ is an average over the baroclinic zone, $\overline{\theta}$ is the zonal and time mean potential temperature, $\sigma_t$ is the lowest level of the tropopause in the baroclinic zone, $p_0 = 10^5$ Pa is a reference surface pressure, and other symbols have their usual meanings (e.g., Holton 2004). The effective MAPE has similar scaling behavior to the dry MAPE over the full range of climates (Fig. 11). Contributing factors to the similar scaling of dry and effective MAPE include the dependence of effective MAPE on the effective static stability throughout the depth of the troposphere (including the relatively dry middle and upper troposphere) and the poleward movement with warming of the storm tracks and baroclinic zones to relatively drier parts of the atmosphere where the effective and dry static stability are similar.

How does the new effective MAPE compare with the moist MAPE of Lorenz (1978, 1979)? We show here that linear scaling with EKE also holds approximately for the moist MAPE (Fig. 11). To calculate the moist MAPE, we first interpolate the zonal- and time-mean temperature and humidity fields to an equal-area grid in latitude (40 latitudes) and an evenly spaced but staggered grid in pressure (40 levels) (cf. Lorenz 1979). We use the original parcel-moving algorithm of Lorenz (1979) rather than the slightly modified version suggested by Randall and Wang (1992) because the original algorithm finds lower-enthalpy reference states for the mean states considered here. Comparing all versions of MAPE, we find that the effective MAPE has a slightly more positive trend with warming than the moist or dry MAPE.

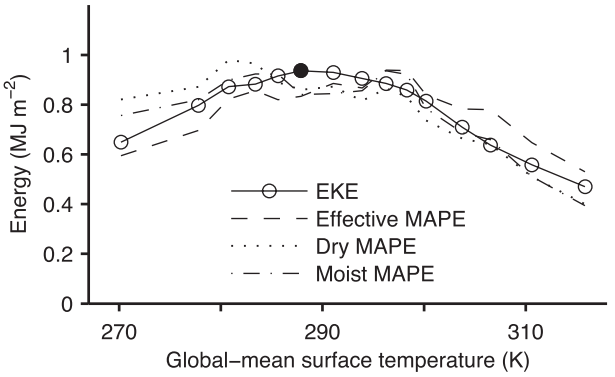


FIG. 11. Column-integrated EKE averaged over the extratropical baroclinic zones in a wide range of climates in the idealized GCM (solid line and circles). Also shown are the rescaled effective MAPE (dashed), dry MAPE (dotted), and moist MAPE (dashed–dotted). Multiplicative rescaling constants are chosen by a least squares fit to the EKE curve, with values of 1.5 (effective MAPE), 2.4 (dry MAPE), and 1.5 (moist MAPE). The dry and effective MAPE are calculated using the quadratic approximation of Lorenz (1955), whereas the moist MAPE is calculated using a parcel-moving algorithm. Similar scaling of the dry MAPE is obtained (i.e., up to a constant multiplicative factor) if it is instead calculated using a parcel moving algorithm. However, the apparent agreement between the rescaling constants for the effective and moist MAPE is coincidental because they are not both calculated using the quadratic approximation. A constant value of $\lambda = 0.6$ is used in the effective MAPE calculation.

The primary disadvantage of the moist MAPE is that there is no approximation of the moist MAPE comparable to the quadratic approximation of Lorenz (1955). Instead it must be calculated numerically (or graphically), making it also more difficult to interpret. The new effective MAPE also takes account of latent heat release but should be much easier to calculate and interpret than the moist MAPE. The similar scaling of dry, effective, and moist MAPE in the extratropics suggests that latent heat release does not strongly energize large-scale extratropical eddies in a warmer atmosphere, at least in this "aquaplanet" setting.

### d. Extratropical eddy length

The extratropical eddy length has increased in the Southern Hemisphere in recent decades according to

[4] We calculate all energies over the baroclinic zones, as defined in footnote 2. Using global averages would change the behavior of the MAPE, as discussed in O'Gorman and Schneider (2008a). All versions of MAPE are calculated between $\sigma = 0.9$ and the lowest level of the tropopause in the baroclinic zones.

reanalysis data, and it also increases in simulations of global warming scenarios (Kidston et al. 2010). We characterize the eddy length in the idealized GCM simulations using a spherical wavenumber $n_e$, defined by

$$n_e(n_e + 1) = \frac{\sum_n E_n}{\sum_n [n(n+1)]^{-1} E_n}, \tag{17}$$

where the eddy kinetic energy spectrum $E_n$ involves a summation over all zonal wavenumbers except zero (Boer and Shepherd 1983; Schneider and Walker 2006).[5] The spherical wavenumber $n_e$ is converted into the corresponding eddy length using $L_e = 2\pi a[n_e(n_e + 1)]^{-1/2}$, where $a$ is the radius of the earth. The eddy length does not change greatly over the range of climates simulated, although it does increase somewhat in very warm climates (Fig. 12).

The atmosphere does not exhibit a substantial inverse energy cascade beyond the length scale associated with conversion to eddy kinetic energy, and so we expect that the eddy length will be related to the characteristic length scale of baroclinic instability (although the eddy length does not generally give the maximum linear growth rate; Pedlosky 1981; Merlis and Schneider 2009). Indeed, the eddy length was found to scale with the Rossby radius over a wide range of simulations with an idealized dry GCM (Schneider and Walker 2006).

We compare the changes in the dry Rossby radius and a new effective Rossby radius with the changes in the eddy length in the moist idealized simulations. The effective Rossby radius is calculated as

$$R_{\text{eff}} = 2\pi \frac{N^p_{\text{eff}} \Delta_p}{f}, \tag{18}$$

where $\Delta_p$ is the pressure depth of the troposphere, the numerator is averaged over the baroclinic zones, and the Coriolis parameter $f$ is evaluated at the centers of the baroclinic zones.[6] The effective static stability parameter

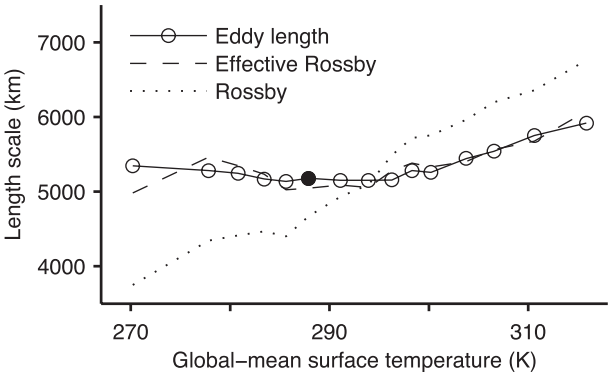


FIG. 12. Eddy length in a wide range of climates in the idealized GCM (solid line and circles). Also shown are the effective Rossby radius (dashed) and the dry Rossby radius (dotted). The Rossby radii have been rescaled by multiplicative constants determined by a least squares fit to the eddy length (1.75 for the effective radius and 1.23 for the dry radius). A constant value of $\lambda = 0.6$ is used in the effective Rossby radius calculation.

$N^p_{\text{eff}} = (-\overline{\partial\theta/\partial p}_{\text{eff}})^{1/2}(\overline{\rho}\overline{\theta})^{-1/2}$ is evaluated near the surface (vertically averaged from $\sigma = 0.8$ to 0.7).

The effective Rossby radius scales with the eddy length over the full range of climates simulated (Fig. 12). The dry Rossby radius is calculated in the same way except using the dry static stability instead of the effective static stability; it does not scale with the eddy length (Fig. 12) but rather increases monotonically as the climate warms, primarily because of the increasing depth of the troposphere. The Rhines scale was also calculated, and while it does not give as good agreement with the eddy length as the effective Rossby radius, it does capture the relative invariance of the eddy length as the climate changes (not shown).

If the eddy length scales with the dry Rossby radius, then it seems reasonable to expect an increasing eddy length as the climate warms because of the increasing dry static stability and depth of the troposphere. But our results suggest that the eddy length scales with the effective Rossby radius rather than the dry Rossby radius. In the idealized simulations, the effective static stability first decreases and then remains relatively constant as the climate warms (the effective static stability is the difference between the dry static stability and the lower gray line in Fig. 9). Therefore, it is no longer obvious that the eddy length should increase with warming, since the changes in effective static stability could compensate for the increasing depth of the troposphere.

## 8. Conclusions

We have derived an effective static stability that to leading order converts dry eddy dynamics to moist eddy dynamics. We have also shown that the eddy statistics in

[5] Use of the eddy kinetic energy spectrum of only barotropic motions as in Schneider and Walker (2006) gives similar results, but with slightly worse agreement with the effective Rossby radius.

[6] Schneider and Walker (2006) included a supercriticality factor in the definition of the Rossby radius to allow for simulations in which convection controls the height of the extratropical tropopause. We do not include a supercriticality factor because eddy entropy fluxes generally reach to near the level of the tropopause in our moist simulations (Schneider and O'Gorman 2008). Inclusion of a dry supercriticality factor does not improve the agreement between the scaling of the dry Rossby radius and the eddy length, and inclusion of an effective supercriticality factor worsens the agreement between the scaling of the effective Rossby radius and the eddy length.

a simulation with a hydrological cycle cannot be reproduced in a dry simulation with the same mean fields, but they can be reproduced if the static stability in the dry simulation is replaced by the effective static stability. Evaluation based on reanalysis data indicates that the effective static stability is considerably smaller than the dry static stability in the lower troposphere of the tropics and midlatitudes. The effective static stability can be used to modify dry theories involving eddy dynamics to account for the leading-order effects of latent heat release (although it cannot be directly applied to the evolution of the mean flow). Substitution of the effective static stability in dry dynamical theories yields effective theories that correctly account for the behavior of several important features of the general circulation in moist idealized simulations of changed climates. Our results make clear that latent heating is an important factor in the eddy dynamics of the extratropical troposphere in the current climate, a factor that cannot be ignored in theories of the general circulation. Further work is needed to explore the transition from control of the extratropical stratification by eddies coupled to moist convection and large-scale condensation to control by moist convection alone, and whether this corresponds to a change in climate stability as had previously been hypothesized (Schneider and Walker 2008).

The reduction of the effective static stability compared with the dry static stability in the deep tropics is close to consistent with the reduction in the speed of equatorial convectively coupled waves compared with dry waves. Although a relatively crude representation of latent heating is used to derive the effective static stability, the approach presented here does have the merit of taking into account the effect of large-scale nonconvecting regions of waves, unlike theories based on small perturbations to always-convecting atmospheres. It may also be possible to generalize the derivation by using the surface precipitation rate directly rather than using the truncated upward velocity $\omega^{\uparrow}$. Since the tropical free troposphere is close to a moist adiabatic thermal stratification, the effective static stability in the tropics primarily depends on surface temperature and the rescaling coefficient $\lambda$. The expression (5) for $\lambda$ then provides a link between the effective static stability felt by convectively coupled waves and the degree of asymmetry between large-scale ascent and descent regions (or precipitating and nonprecipitating regions) of the waves, although further work would be needed to determine whether the effective static stability is indeed relevant to such waves.

Important questions remain concerning the rescaling coefficient $\lambda$. In particular, why does it have a value of $\lambda \sim 0.6$ in the extratropics, and why does it not increase as the climate warms and the thermal stratification approaches moist adiabatic? This stands in contrast to the behavior of normal modes of moist baroclinic instability in which the updraft area becomes small (or vanishes in some models) in the limit of slantwise-moist-convective neutrality (Emanuel et al. 1987; Fantini 1990; Zurita-Gotor 2005). It remains to be seen if $\lambda$ remains constant as the climate changes in comprehensive GCMs or in nature. There is a slight increase in $\lambda$ when the spatial resolution is doubled in the reference simulation of the idealized GCM, but several other circulation statistics also change, and we leave the values of $\lambda$ and their sensitivity to spatial resolution as a subject for future work.

The primary merit of the effective static stability is in revealing the thermodynamic and dynamic dependencies of the relevant static stability for eddies in a moist atmosphere. As such it is an advance in our understanding of the general circulation and should prove useful in a variety of applications.

*Acknowledgments.* Thanks to Tapio Schneider, Kerry Emanuel, Tim Merlis, Caroline Muller, Marty Singh, and Malte Jansen for helpful comments. NCEP-DOE Reanalysis 2 data were provided by the NOAA/OAR/ESRL PSD (see http://www.esrl.noaa.gov/psd/). The idealized GCM simulations were performed on Caltech's Division of Geological and Planetary Sciences Dell cluster.

## APPENDIX

### Approximation of Latent Heating Rate

A preliminary step in the derivation of the effective static stability involves approximating the latent heating rate in terms of the truncated upward vertical, as given by the second term on the right-hand side of Eq. (3). We evaluate the accuracy of this approximation using 4-times-daily NCEP-2 reanalysis data (vertical velocities are reported as instantaneous values, but precipitation rates are 6-hourly averages). Surface precipitation rates are compared with the mass-weighted vertical integral of $\omega^{\uparrow}(T/\theta)\overline{\partial\theta/\partial p|_{\theta^*}}c_p/L$, where $c_p$ is the specific heat capacity of air, $L$ is the latent heat of condensation, and the overbar denotes a zonal average. The standard deviation of the approximate precipitation rate is consistently too low by about 20% (Fig. A1). An alternative approximation is also evaluated in which the zonal mean of the moist adiabatic derivative $\partial\theta/\partial p|_{\theta^*}$ is not taken (dashed–dotted line in Fig. A1). Comparison of the two approximations indicates that roughly half of the discrepancy in the extratropics is attributable to the neglect of correlations between the vertical velocity and eddy variations of the moist adiabatic derivative. These correlations make a positive contribution because upward motion is associated

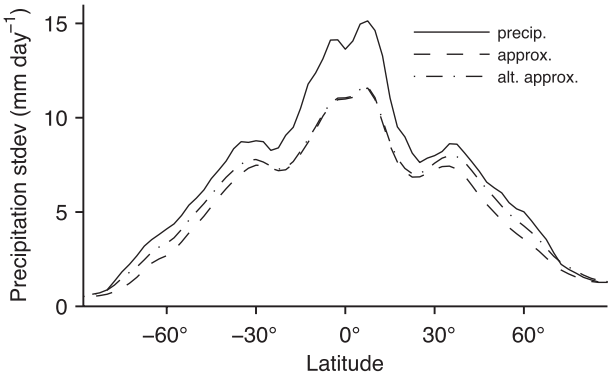


FIG. A1. Standard deviations of the surface precipitation rate (solid) and an approximate precipitation rate (dashed) consistent with the approximate latent heating expression in Eq. (3). Also shown is an alternative approximation in which the eddy variations in the moist adiabatic derivative of potential temperature are not neglected (dashed–dotted). The standard deviations are based on time and zonal means of 4-times-daily fields from the NCEP-2 reanalysis (1992–2001). A 1–2–1 filter in latitude was applied to the results for clarity.

with the warm regions of eddies, a factor that could be taken into account at the expense of additional complexity in the definition of the effective static stability.

The correlation coefficient between the actual and approximate 4-times-daily precipitation rates evaluated at all latitudes and longitudes has a global-mean value of 0.60. This relatively low value is partly due to using instantaneous vertical velocity data but 6-hourly-average precipitation data. A higher global-mean correlation coefficient of 0.76 is obtained when daily-mean data are used for both the vertical velocities and precipitation rates, and it would likely be greater again if instantaneous values were used for both fields.

The comparison based on precipitation rates suggests that this approximation may lead to an underestimation of the importance of latent heating in the effective static stability based on reanalysis data. But the precipitation rate is only representative of the column-integrated latent heating rate, and so a different bias may occur at a given level of the atmosphere. A similar level of accuracy is found for this approximation in the idealized GCM simulations (not shown).

## REFERENCES


Bengtsson, L., K. I. Hodges, and N. Keenlyside, 2009: Will extratropical storms intensify in a warmer climate? *J. Climate,* **22,** 2276–2301.

Bjerknes, J., 1938: Saturated-adiabatic ascent of air through dry-adiabatically descending environment. *Quart. J. Roy. Meteor. Soc.,* **64,** 325–330.

Boer, G. J., and T. G. Shepherd, 1983: Large-scale two-dimensional turbulence in the atmosphere. *J. Atmos. Sci.,* **40,** 164–184.

Chang, E. K. M., 2006: An idealized nonlinear model of the Northern Hemisphere winter storm tracks. *J. Atmos. Sci.,* **63,** 1818–1839.

——, S. Lee, and K. L. Swanson, 2002: Storm track dynamics. *J. Climate,* **15,** 2163–2183.

Emanuel, K. A., 1994: *Atmospheric Convection*. Oxford University Press, 580 pp.

——, M. Fantini, and A. J. Thorpe, 1987: Baroclinic instability in an environment of small stability to slantwise moist convection. Part I: Two-dimensional models. *J. Atmos. Sci.,* **44,** 1559–1573.

Fantini, M., 1990: Nongeostrophic corrections to the eigensolutions of a moist baroclinic instability problem. *J. Atmos. Sci.,* **47,** 1277–1287.

Frierson, D. M. W., 2007: The dynamics of idealized convection schemes and their effect on the zonally averaged tropical circulation. *J. Atmos. Sci.,* **64,** 1959–1976.

——, 2008: Midlatitude static stability in simple and comprehensive general circulation models. *J. Atmos. Sci.,* **65,** 1049–1062.

Geng, Q., and M. Sugi, 2003: Possible change of extratropical cyclone activity due to enhanced greenhouse gases and sulfate aerosols—Study with a high-resolution AGCM. *J. Climate,* **16,** 2262–2274.

Gutowski, W. J., Jr., 1985: Baroclinic adjustment and midlatitude temperature profiles. *J. Atmos. Sci.,* **42,** 1733–1745.

——, L. E. Branscome, and D. A. Stewart, 1992: Life cycles of moist baroclinic eddies. *J. Atmos. Sci.,* **49,** 306–319.

Hall, N. M. J., B. J. Hoskins, P. J. Valdes, and C. A. Senior, 1994: Storm tracks in a high-resolution GCM with doubled carbon dioxide. *Quart. J. Roy. Meteor. Soc.,* **120,** 1209–1230.

Held, I. M., 2000: The general circulation of the atmosphere. *Proc. Prog. Geophys. Fluid Dyn.,* Woods Hole Oceanographic Institute, Woods Hole, MA. [Available online at http://hdl.handle.net/1912/15.]

Holton, J. R., 2004: *An Introduction to Dynamic Meteorology*. 4th ed. Elsevier Academic, 535 pp.

Juckes, M. N., 2000: The static stability of the midlatitude troposphere: The relevance of moisture. *J. Atmos. Sci.,* **57,** 3050–3057.

Kanamitsu, M., W. Ebisuzaki, J. Woollen, S. K. Yang, J. J. Hnilo, M. Fiorino, and G. L. Potter, 2002: NCEP-DOE AMIP-II Reanalysis (R-2). *Bull. Amer. Meteor. Soc.,* **83,** 1631–1643.

Kidston, J., S. M. Dean, J. A. Renwick, and G. K. Vallis, 2010: A robust increase in the eddy length scale in the simulation of future climates. *Geophys. Res. Lett.,* **37,** L03806, doi:10.1029/2009GL041615.

Kiladis, G. N., M. C. Wheeler, P. T. Haertel, K. H. Straub, and P. E. Roundy, 2009: Convectively coupled equatorial waves. *Rev. Geophys.,* **47,** RG2003, doi:10.1029/2008RG000266.

Korty, R. L., and T. Schneider, 2008: Extent of Hadley circulations in dry atmospheres. *Geophys. Res. Lett.,* **35,** L23803, doi:10.1029/2008GL035847.

Lapeyre, G., and I. M. Held, 2004: The role of moisture in the dynamics and energetics of turbulent baroclinic eddies. *J. Atmos. Sci.,* **61,** 1693–1710.

Lorenz, E. N., 1955: Available potential energy and the maintenance of the general circulation. *Tellus,* **7,** 157–167.

——, 1978: Available energy and the maintenance of a moist circulation. *Tellus,* **30,** 15–31.

——, 1979: Numerical evaluation of moist available energy. *Tellus,* **31,** 230–235.

Lu, J., G. A. Vecchi, and T. Reichler, 2007: Expansion of the Hadley cell under global warming. *Geophys. Res. Lett.,* **34,** L06805, doi:10.1029/2006GL028443.

Merlis, T. M., and T. Schneider, 2009: Scales of linear baroclinic instability and macroturbulence in dry atmospheres. *J. Atmos. Sci.,* **66,** 1821–1833.

Neelin, J. D., and I. M. Held, 1987: Modeling tropical convergence based on the moist static energy budget. *Mon. Wea. Rev.,* **115,** 3–12.

——, ——, and K. H. Cook, 1987: Evaporation–wind feedback and low-frequency variability in the tropical atmosphere. *J. Atmos. Sci.,* **44,** 2341–2348.

O'Gorman, P. A., and T. Schneider, 2006: Stochastic models for the kinematics of moisture transport and condensation in homogeneous turbulent flows. *J. Atmos. Sci.,* **63,** 2992–3005.

——, and ——, 2007: Recovery of atmospheric flow statistics in a general circulation model without nonlinear eddy–eddy interactions. *Geophys. Res. Lett.,* **34,** L22801, doi:10.1029/2007GL031779.

——, and ——, 2008a: Energy of midlatitude transient eddies in idealized simulations of changed climates. *J. Climate,* **21,** 5797–5806.

——, and ——, 2008b: The hydrological cycle over a wide range of climates simulated with an idealized GCM. *J. Climate,* **21,** 3815–3832.

——, and ——, 2009a: The physical basis for increases in precipitation extremes in simulations of 21st-century climate change. *Proc. Natl. Acad. Sci. USA,* **106,** 14 773–14 777.

——, and ——, 2009b: Scaling of precipitation extremes over a wide range of climates simulated with an idealized GCM. *J. Climate,* **22,** 5676–5685.

——, and C. J. Muller, 2010: How closely do changes in surface and column water vapor follow Clausius–Clapeyron scaling in climate-change simulations? *Environ. Res. Lett.,* **5,** 025207, doi:10.1088/1748-9326/5/2/025207.

Pedlosky, J., 1981: The nonlinear dynamics of baroclinic wave ensembles. *J. Fluid Mech.,* **102,** 169–209.

Randall, D. A., and J. Wang, 1992: The moist available energy of a conditionally unstable atmosphere. *J. Atmos. Sci.,* **49,** 240–255.

Reed, R. J., A. J. Simmons, M. D. Albright, and P. Undén, 1988: The role of latent heat release in explosive cyclogenesis: Three examples based on ECMWF operational forecasts. *Wea. Forecasting,* **3,** 217–229.

Schneider, T., and C. C. Walker, 2006: Self-organization of atmospheric macroturbulence into critical states of weak nonlinear eddy–eddy interactions. *J. Atmos. Sci.,* **63,** 1569–1586.

——, and P. A. O'Gorman, 2008: Moist convection and the thermal stratification of the extratropical troposphere. *J. Atmos. Sci.,* **65,** 3571–3583.

——, and C. C. Walker, 2008: Scaling laws and regime transitions of macroturbulence in dry atmospheres. *J. Atmos. Sci.,* **65,** 2153–2173.

——, P. A. O'Gorman, and X. Levine, 2010: Water vapor and the dynamics of climate changes. *Rev. Geophys.,* **48,** RG3001, doi:10.1029/2009RG000302.

Seidel, D. J., Q. Fu, W. J. Randel, and T. J. Reichler, 2008: Widening of the tropical belt in a changing climate. *Nat. Geosci.,* **1,** 21–24.

Stone, P. H., 1978: Baroclinic adjustment. *J. Atmos. Sci.,* **35,** 561–571.

Thuburn, J., and G. C. Craig, 1997: GCM tests of theories for the height of the tropopause. *J. Atmos. Sci.,* **54,** 869–882.

Trenberth, K. E., and D. P. Stepaniak, 2003: Covariability of components of poleward atmospheric energy transports on seasonal and interannual timescales. *J. Climate,* **16,** 3691–3705.

Wheeler, M., and G. N. Kiladis, 1999: Convectively coupled equatorial waves: Analysis of clouds and temperature in the wavenumber–frequency domain. *J. Atmos. Sci.,* **56,** 374–399.

Yano, J., and K. Emanuel, 1991: An improved model of the equatorial troposphere and its coupling with the stratosphere. *J. Atmos. Sci.,* **48,** 377–389.

Yin, J. H., 2005: A consistent poleward shift of the storm tracks in simulations of 21st century climate. *Geophys. Res. Lett.,* **32,** L18701, doi:10.1029/2005GL023684.

Zhou, S., and P. H. Stone, 1993: The role of large-scale eddies in the climate equilibrium. Part II: Variable static stability. *J. Climate,* **6,** 1871–1881.

Zurita-Gotor, P., 2005: Updraft/downdraft constraints for moist baroclinic modes and their implications for the short-wave cutoff and maximum growth rate. *J. Atmos. Sci.,* **62,** 4450–4458.

——, and R. S. Lindzen, 2007: Theories of baroclinic adjustment and eddy equilibration. *The Global Circulation of the Atmosphere,* T. Schneider and A. H. Sobel, Eds., Princeton University Press, 22–46.